Adaptive Feedback Linearization Control Based on Airgap Flux Model for Induction Motors

Seok Ho Jeon, Dane Baang, and Jin Young Choi*

Abstract: This paper presents an adaptive feedback linearization control scheme for induction motors with simultaneous variation of rotor and stator resistances. Two typical modeling techniques, rotor flux model and stator flux model, have been developed and successfully applied to the controller design and adaptive observer design, respectively. By using stator fluxes as states, over-parametrization in adaptive control can be prevented and control strategy can be developed without the need of nonlinear transformation. It also decrease the relative degree for the flux modulus by one, thereby, yielding a simple control algorithm. However, when this method is used for flux observer, it cannot guarantee the convergence of flux. Similarly, the rotor flux model may be appropriate for observers, but it is not so for adaptive controllers. In addition, if these two existing methods are merged into overall adaptive control system, it brings about structural complexies. In this paper, we did not use these two medeling methods, and opted for the airgap flux model which takes on only the positive aspects of the existing rotor flux model and stator flux model and prevents structural complexity from occuring. Through theoretical analysis by using Lyapunov's direct method, simulations, and actual experiments, it is shown that stator and rotor resistances converge to their actual values, flux is well estimated, and torque and flux are controlled independently with the measurements of rotor speed, stator currents, and stator voltages. These results were achieved under the persistent excitation condition, which is shown to hold in the simulation.

Keywords: Adaptive control, adaptive observer, feedback linearization, induction motors, parameter estimation.

1. INTRODUCTION

The field-oriented control scheme has been developed to achieve high performance of induction motors that are widely used in industry due to its reliability, low cost, and easy maintenance. While there are flux changes, the field-oriented control scheme cannot achieve decoupling control between two output variables (i.e., torque and flux). Furthermore, there are certain motor parameters such as rotor resistance and stator resistance that tend to vary during operation due to temperature, skin effect, etc, and so it is necessary to find means to compensate for such variations. Many researches have been conducted to estimate the rotor and stator resistances, such as using MRAC (Model reference adaptive control) [1-4], extended kalman filter [5-10], neural network and fuzzy logic [11-13]. But in most of these techniques, it is assume that at least one of rotor resistance or stator resistance is known.

Various nonlinear control schemes have also been applied to induction motors. In particular, the feedback linearization methods that guarantee the decoupling characteristics for all operation regions have been proposed [7-15]. Passivity-based methods have been applied to induction motors [16-18] and the backstepping technique has also been proposed [19]. In order to estimate both resistances and control torque and flux, there are two kinds of modeling methods, but they both have good and bad points.

By using stator fluxes as states, over-parametrization in adaptive control can be prevented and control inputs can be determined directly without the need of nonlinear transformation. With this approach, the relative degree for the flux modulus can be decreased, hence, yielding a simple control algorithm. But, when this method is used for flux observer, it cannot guarantee the convergence of flux. By using rotor fluxes as states, it can be guaranteed that the asymptotic convergence of flux is achieved when used for flux observers. On the hindsight, however, over-parametrization is unavoidable, relative

Manuscript received August 1, 2005; revised January 13, 2006; accepted April 6, 2006. Recommended by Editor Keum-Shik Hong.

Seok Ho Jeon, Dane Baang, and Jin Young Choi are with the School of Electrical Engineering and Computer Science, Seoul National University, Kwanak P.O.Box 34, Seoul 151-742, Korea (e-mails: {shjeon, dibang, jychoi}@neuro.snu.ac.kr).

* Corresponding author.

degree for the flux modulus is not decreased, and lastly, a nonlinear transformation is needed in adaptive control problem.

In summary, stator flux model may be appropriate for controller design and rotor flux model for observer design, but a combined control system that uses the stator flux model for controller and rotor flux model for observer, involve extremely complex structure and equations. To overcome this limitation, in this paper, we propose an adaptive input-output feedback linearization control system based on the airgap flux model, which takes on only the positive aspects of the two models and at the same time assures that the design of both controller and observer are not much complex. The overall stability and convergence analysis by using Lyapunov's direct method shows that, under the persistent excitation condition, the proposed adaptive observer can estimate correct values of stator and rotor resistances as well as airgap flux in the case of simultaneous variation of stator and rotor resistances. Torque and flux can be controlled independently with the measurements of rotor speed, stator currents and stator voltages. Through computer simulations and actual experiments, the effectiveness of the proposed control scheme is verified.

The rest of the paper is organized as follows. In Section 2, we will describe the modeling methods and derive error dynamics. In Section 3, we will design torque and flux controllers. In Section 4, we will derive adaptive laws and present the result of the overall convergence analysis. In Section 5 and 6, we present the simulation results and experiment results, respectively. Finally, in Section 7, we present our conclusions.

2. MODELING AND ERROR DYNAMICS DERIVATION

Using dq-transformation, the electrical dynamics of a three-phase induction motor can be described in a two-axis coordinates frame [2]. If we choose a stationary reference frame, it is described as

$$\begin{aligned}
V_{ds} &= R_s i_{ds} + \frac{d}{dt}\lambda_{ds}, \\
V_{qs} &= R_s i_{qs} + \frac{d}{dt}\lambda_{qs}, \\
0 &= R_r i_{dr} + \frac{d}{dt}\lambda_{dr} + \omega_r \lambda_{qr}, \\
0 &= R_r i_{qr} + \frac{d}{dt}\lambda_{qr} - \omega_r \lambda_{dr}.
\end{aligned} \tag{1}$$

The first two in (1) are stator circuit equations and the rest are rotor circuit equations. The relation between fluxes and currents are given by (2), under the assumption of linear magnetic circuits.

$$\begin{aligned}
\lambda_{ds} &= L_{ls} i_{ds} + L_m (i_{ds} + i_{dr}) = L_s i_{ds} + L_m i_{dr}, \\
\lambda_{qs} &= L_{ls} i_{qs} + L_m (i_{qs} + i_{qr}) = L_s i_{qs} + L_m i_{qr}, \\
\lambda_{dr} &= L_{lr} i_{dr} + L_m (i_{ds} + i_{dr}) = L_r i_{dr} + L_m i_{ds}, \\
\lambda_{qr} &= L_{lr} i_{qr} + L_m (i_{qs} + i_{qr}) = L_r i_{qr} + L_m i_{qs}, \\
\lambda_{da} &= L_m (i_{ds} + i_{dr}), \\
\lambda_{qa} &= L_m (i_{qs} + i_{qr}).
\end{aligned} \tag{2}$$

Among the variables, if we choose airgap fluxes $\lambda_{da}, \lambda_{qa}$ as states, the airgap flux model is given by (3).

Airgap flux model:

$$\begin{aligned}
\frac{d}{dt}\lambda_{da} &= \frac{L_{ls} - L_\sigma}{L_\sigma} R_s i_{ds} - \frac{L_{ls}}{L_r L_\sigma} R_r \lambda_{da} + \frac{L_{ls} L_m}{L_r L_\sigma} R_r i_{ds} \\
&\quad - \frac{L_{ls}}{L_\sigma}\omega_r \lambda_{qa} - \frac{L_{ls}}{L_\sigma}(L_{ls} - L_\sigma)\omega_r i_{qs} - \frac{L_{ls} - L_\sigma}{L_\sigma} V_{ds} \\
\frac{d}{dt}\lambda_{qa} &= \frac{L_{ls} - L_\sigma}{L_\sigma} R_s i_{qs} - \frac{L_{ls}}{L_r L_\sigma} R_r \lambda_{qa} + \frac{L_{ls} L_m}{L_r L_\sigma} R_r i_{qs} \\
&\quad + \frac{L_{ls}}{L_\sigma}\omega_r \lambda_{da} + \frac{L_{ls}}{L_\sigma}(L_{ls} - L_\sigma)\omega_r i_{ds} - \frac{L_{ls} - L_\sigma}{L_\sigma} V_{qs} \\
\frac{d}{dt} i_{ds} &= -\frac{R_s}{L_\sigma} i_{ds} + \frac{R_r}{L_r L_\sigma}(\lambda_{da} - L_m i_{ds}) \\
&\quad + \frac{1}{L_\sigma}\omega_r \lambda_{qa} + \frac{L_{ls} - L_\sigma}{L_\sigma}\omega_r i_{qs} + \frac{1}{L_\sigma} V_{ds}, \\
\frac{d}{dt} i_{qs} &= -\frac{R_s}{L_\sigma} i_{qs} + \frac{R_r}{L_r L_\sigma}(\lambda_{qa} - L_m i_{qs}) \\
&\quad - \frac{1}{L_\sigma}\omega_r \lambda_{da} - \frac{L_{ls} - L_\sigma}{L_\sigma}\omega_r i_{ds} + \frac{1}{L_\sigma} V_{qs}.
\end{aligned} \tag{3}$$

In most cases, i_{ds}, i_{qs} can be directly measurable, but $\lambda_{da}, \lambda_{qa}$ can not, which means an observer is necessary. If the Luenberger observer is used, assuming that the information of all parameter values are provided, the dynamics of the error between the estimated flux and the real flux can be easily assured to be globally asymptotically stable as follows.

Flux estimation law:

$$\begin{aligned}
\frac{d}{dt}\lambda_{da} &= \frac{L_{ls} - L_\sigma}{L_\sigma} R_s i_{ds} - \frac{L_{ls}}{L_r L_\sigma} R_r \hat{\lambda}_{da} + \frac{L_{ls} L_m}{L_r L_\sigma} R_r i_{ds} \\
&\quad - \frac{L_{ls}}{L_\sigma}\omega_r \hat{\lambda}_{qa} - \frac{L_{ls}}{L_\sigma}(L_{ls} - L_\sigma)\omega_r i_{qs} - \frac{L_{ls} - L_\sigma}{L_\sigma} V_{ds}, \\
\frac{d}{dt}\lambda_{qa} &= \frac{L_{ls} - L_\sigma}{L_\sigma} R_s i_{qs} - \frac{L_{ls}}{L_r L_\sigma} R_r \hat{\lambda}_{qa} + \frac{L_{ls} L_m}{L_r L_\sigma} R_r i_{qs} \\
&\quad + \frac{L_{ls}}{L_\sigma}\omega_r \hat{\lambda}_{da} + \frac{L_{ls}}{L_\sigma}(L_{ls} - L_\sigma)\omega_r i_{ds} - \frac{L_{ls} - L_\sigma}{L_\sigma} V_{qs},
\end{aligned} \tag{4}$$

where $\hat{\lambda}_{da}, \hat{\lambda}_{qa}$ are estimates of $\lambda_{da}, \lambda_{qa}$, respectively.

Flux estimation error:

$$\frac{d}{dt}\tilde{\lambda}_{da} = -\frac{L_{ls}}{L_r L_\sigma} R_r \tilde{\lambda}_{da} - \frac{L_{ls}}{L_\sigma}\omega_r \tilde{\lambda}_{qa},$$
$$\frac{d}{dt}\tilde{\lambda}_{qa} = -\frac{L_{ls}}{L_r L_\sigma} R_r \tilde{\lambda}_{qa} + \frac{L_{ls}}{L_\sigma}\omega_r \tilde{\lambda}_{da}, \tag{5}$$

where $\tilde{\lambda}_{da} \triangleq \lambda_{da} - \hat{\lambda}_{da}$, $\tilde{\lambda}_{qa} \triangleq \lambda_{qa} - \hat{\lambda}_{qa}$.

Define Lyapunov-like function as $V_a = \frac{1}{2}\left(\tilde{\lambda}_{da}^2 + \tilde{\lambda}_{qa}^2\right)$, then its derivative is $\frac{d}{dt}V_a = -\frac{L_{ls}R_r}{L_r L_\sigma}\left(\tilde{\lambda}_{da}^2 + \tilde{\lambda}_{qa}^2\right)$. So $\left[\tilde{\lambda}_{da}, \tilde{\lambda}_{qa}\right] \in L_\infty \cap L_2$ and, from (5), $\left[\dot{\tilde{\lambda}}_{da}, \dot{\tilde{\lambda}}_{qa}\right] \in L_\infty$. From Barbalat's Lemma [20], we can derive $\lim_{t\to\infty} \tilde{\lambda}_{da} = 0$, $\lim_{t\to\infty} \tilde{\lambda}_{qa} = 0$.

The problem that is dealt with in this paper, is the feedback linearizing controller design when R_s, R_r are bounded constants, but unknown. In such case, an adaptive observer which estimates R_s, R_r, and λ_{da}, λ_{qa} simultaneously is needed. The proposed adaptive observer for dealing with these estimations has the following form, with R_s, R_r, replaced by there corresponding estimates, respectively, and two additional design functions f_d, f_q.

$$\frac{d}{dt}\hat{\lambda}_{da} = \frac{L_{ls} - L_\sigma}{L_\sigma}\hat{R}_s i_{ds} - \frac{L_{ls}}{L_r L_\sigma}(\hat{\lambda}_{da} - L_m i_{ds})\hat{R}_r$$
$$-\frac{L_{ls}}{L_\sigma}\omega_r \hat{\lambda}_{qa} - \frac{L_{ls}}{L_\sigma}(L_{ls} - L_\sigma)\omega_r i_{qs} - \frac{L_{ls} - L_\sigma}{L_\sigma}V_{ds},$$
$$\frac{d}{dt}\hat{\lambda}_{qa} = \frac{L_{ls} - L_\sigma}{L_\sigma}\hat{R}_s i_{qs} - \frac{L_{ls}}{L_r L_\sigma}(\hat{\lambda}_{qa} - L_m i_{qs})\hat{R}_r$$
$$+\frac{L_{ls}}{L_\sigma}\omega_r \hat{\lambda}_{da} + \frac{L_{ls}}{L_\sigma}(L_{ls} - L_\sigma)\omega_r i_{ds} - \frac{L_{ls} - L_\sigma}{L_\sigma}V_{qs},$$
$$\frac{d}{dt}\hat{i}_{ds} = -\frac{\hat{R}_s}{L_\sigma}i_{ds} + \frac{\hat{R}_r}{L_r L_\sigma}(\hat{\lambda}_{da} - L_m i_{ds})$$
$$+\frac{1}{L_\sigma}\omega_r \hat{\lambda}_{qa} + \frac{L_{ls} - L_\sigma}{L_\sigma}\omega_r i_{qs} + \frac{1}{L_\sigma}V_{ds} + f_d, \tag{6}$$
$$\frac{d}{dt}\hat{i}_{qs} = -\frac{\hat{R}_s}{L_\sigma}i_{qs} + \frac{\hat{R}_r}{L_r L_\sigma}(\hat{\lambda}_{qa} - L_m i_{qs})$$
$$-\frac{1}{L_\sigma}\omega_r \hat{\lambda}_{da} - \frac{L_{ls} - L_\sigma}{L_\sigma}\omega_r i_{ds} + \frac{1}{L_\sigma}V_{qs} + f_q,$$

where $\hat{i}_{ds}$, $\hat{i}_{qs}$ are estimates of i_{ds}, i_{qs}, respectively.

Since i_{ds}, i_{qs} are measurable, we can practically use them instead of their estimates. But their estimates are used to compose (6) for obtaining error dynamics. This error dynamics will be included in parameter estimation algorithm, where parameters are updated in such a way that it minimizes a function of the errors between the measurable signal (i_{ds}, i_{qs}), and the estimates of them ($\hat{i}_{ds}$, $\hat{i}_{qs}$). From (3) and (6), the error dynamics is given by (7).

$$\frac{d}{dt}\tilde{\lambda}_{da} = \frac{L_{ls} - L_\sigma}{L_\sigma}\tilde{R}_s i_{ds} - \frac{L_{ls}}{L_r L_\sigma}R_r \tilde{\lambda}_{da}$$
$$-\frac{L_{ls}}{L_r L_\sigma}\hat{\lambda}_{da}\tilde{R}_r + \frac{L_{ls}L_m}{L_r L_\sigma}i_{ds}\tilde{R}_r - \frac{L_{ls}}{L_\sigma}\omega_r \tilde{\lambda}_{qa},$$
$$\frac{d}{dt}\tilde{\lambda}_{qa} = \frac{L_{ls} - L_\sigma}{L_\sigma}\tilde{R}_s i_{qs} - \frac{L_{ls}}{L_r L_\sigma}R_r \tilde{\lambda}_{qa}$$
$$-\frac{L_{ls}}{L_r L_\sigma}\hat{\lambda}_{qa}\tilde{R}_r + \frac{L_{ls}L_m}{L_r L_\sigma}i_{qs}\tilde{R}_r + \frac{L_{ls}}{L_\sigma}\omega_r \tilde{\lambda}_{da}, \tag{7}$$
$$\frac{d}{dt}\tilde{i}_{ds} = -\frac{\tilde{R}_s}{L_\sigma}i_{ds} + \frac{R_r}{L_r L_\sigma}\tilde{\lambda}_{da} + \frac{\hat{\lambda}_d}{L_r L_\sigma}\tilde{R}_r$$
$$-\frac{L_m}{L_r L_\sigma}i_{ds}\tilde{R}_r + \frac{1}{L_\sigma}\omega_r \tilde{\lambda}_{qa} - f_d,$$
$$\frac{d}{dt}\tilde{i}_{qs} = -\frac{\tilde{R}_s}{L_\sigma}i_{qs} + \frac{R_r}{L_r L_\sigma}\tilde{\lambda}_{qa} + \frac{\hat{\lambda}_q}{L_r L_\sigma}\tilde{R}_r$$
$$-\frac{L_m}{L_r L_\sigma}i_{qs}\tilde{R}_r - \frac{1}{L_\sigma}\omega_r \tilde{\lambda}_{da} - f_q.$$

Define new state variables z_d, z_q as

$$z_d \triangleq \tilde{\lambda}_{da} + L_{ls}\tilde{i}_{ds} + \int_0^t \tilde{R}_s i_{ds} dt,$$
$$z_q \triangleq \tilde{\lambda}_{qa} + L_{ls}\tilde{i}_{qs} + \int_0^t \tilde{R}_s i_{qs} dt. \tag{8}$$

Then the airgap flux estimation error can be rewritten as

$$\tilde{\lambda}_{da} = z_d - L_{ls}\tilde{i}_{ds} - \tilde{R}_s I_{ds} - \int_0^t \dot{\hat{R}}_s I_{ds} dt,$$
$$\tilde{\lambda}_{qa} = z_q - L_{ls}\tilde{i}_{qs} - \tilde{R}_s I_{qs} - \int_0^t \dot{\hat{R}}_s I_{qs} dt,$$
$$I_{ds} = \int_0^t i_{ds} dt, \tag{9}$$
$$I_{qs} = \int_0^t i_{qs} dt.$$

By applying (7) to (9), the estimation error dynamics about i_{ds}, i_{qs} are expressed as

$$\frac{d}{dt}\tilde{i}_{ds} = -\frac{L_{ls}R_r}{L_r L_\sigma}\tilde{i}_{ds} - \frac{\tilde{R}_s}{L_\sigma}(i_{ds} + \omega_r I_{qs})$$

$$+\frac{\tilde{R}_r}{L_rL_\sigma}(\hat{\lambda}_{da}-L_mi_{ds})+\frac{R_r}{L_rL_\sigma}\tilde{z}_d+\frac{R_r}{L_rL_\sigma}(\hat{z}_d+\int_0^t\hat{R}_si_{ds}dt)-\frac{R}{L_rL_\sigma}I_{ds}+\frac{\omega_r}{L_\sigma}z_q-\frac{L_{ls}}{L_\sigma}\omega_r\tilde{i}_{qs}-\frac{\omega_r}{L_\sigma}\int_0^t\dot{\hat{R}}_sI_{qs}dt-f_d,$$

$$\frac{d}{dt}\tilde{i}_{qs}=-\frac{L_{ls}R_r}{L_rL_\sigma}\tilde{i}_{qs}-\frac{\tilde{R}_s}{L_\sigma}(i_{qs}-\omega_rI_{ds})+\frac{\tilde{R}_r}{L_rL_\sigma}(\hat{\lambda}_{qa}-L_mi_{qs})+\frac{R_r}{L_rL_\sigma}\tilde{z}_q+\frac{R_r}{L_rL_\sigma}(\hat{z}_q+\int_0^t\hat{R}_si_{qs}dt)-\frac{R}{L_rL_\sigma}I_{qs}-\frac{\omega_r}{L_\sigma}z_d+\frac{L_{ls}}{L_\sigma}\omega_r\tilde{i}_{ds}+\frac{\omega_r}{L_\sigma}\int_0^t\dot{\hat{R}}_sI_{ds}dt-f_q,\quad(10)$$

where $R\triangleq R_r\cdot R_s$, $\tilde{z}_d\triangleq z_d-\hat{z}_d$, $\tilde{z}_q\triangleq z_q-\hat{z}_q$. Now we design feedback stabilizing functions f_d, f_q as follows.

$$\begin{aligned}f_d&=\frac{\hat{R}_r}{L_rL_\sigma}(\hat{z}_d+\int_0^t\hat{R}_si_{ds}dt)-\frac{\hat{R}}{L_rL_\sigma}I_{ds}+\frac{\omega_r}{L_\sigma}\hat{z}_q+\frac{\omega_r}{L_\sigma}\hat{\eta}_q-\frac{L_{ls}}{L_\sigma}\omega_r\tilde{i}_{qs}-\frac{\omega_r}{L_\sigma}\int_0^t\dot{\hat{R}}_sI_{qs}dt+k_1\tilde{i}_{ds},\\f_q&=\frac{\hat{R}_r}{L_rL_\sigma}(\hat{z}_q+\int_0^t\hat{R}_si_{qs}dt)-\frac{\hat{R}}{L_rL_\sigma}I_{qs}-\frac{\omega_r}{L_\sigma}\hat{z}_d-\frac{\omega_r}{L_\sigma}\hat{\eta}_d+\frac{L_{ls}}{L_\sigma}\omega_r\tilde{i}_{ds}+\frac{\omega_r}{L_\sigma}\int_0^t\dot{\hat{R}}_sI_{ds}dt+k_2\tilde{i}_{qs},\end{aligned}\quad(11)$$

where k_1, k_2 are some positive gains, η_d, η_q are defined as $\eta_d\triangleq\tilde{z}_d=z_d-\hat{z}_d$, $\eta_q\triangleq\tilde{z}_q=z_q-\hat{z}_q$. η_d, η_q are defined again because the error dynamics of η_d, η_q will be used to derive adaptive laws later on. Finally, by using (11), the estimation of error dynamics for i_{ds}, i_{qs} is obtained as

$$\begin{aligned}\frac{d}{dt}\tilde{i}_{ds}&=-(\frac{L_{ls}R_r}{L_rL_\sigma}+k_1)\tilde{i}_{ds}-\frac{\tilde{R}_s}{L_\sigma}(i_{ds}+\omega_rI_{qs})+\frac{\tilde{R}_r}{L_rL_\sigma}(\hat{\lambda}_{da}-L_mi_{ds}+\hat{z}_d+\int_0^t\hat{R}_si_{ds}dt)+\frac{R_r}{L_rL_\sigma}\tilde{z}_d-\frac{\tilde{R}}{L_rL_\sigma}I_{ds}+\frac{\omega_r}{L_\sigma}\tilde{\eta}_q,\\\frac{d}{dt}\tilde{i}_{qs}&=-(\frac{L_{ls}R_r}{L_rL_\sigma}+k_2)\tilde{i}_{qs}-\frac{\tilde{R}_s}{L_\sigma}(i_{qs}-\omega_rI_{ds})+\frac{\tilde{R}_r}{L_rL_\sigma}(\hat{\lambda}_{qa}-L_mi_{qs}+\hat{z}_q+\int_0^t\hat{R}_si_{qs}dt)+\frac{R_r}{L_rL_\sigma}\tilde{z}_q-\frac{\tilde{R}}{L_rL_\sigma}I_{qs}-\frac{\omega_r}{L_\sigma}\tilde{\eta}_d,\end{aligned}\quad(12)$$

where $\tilde{\eta}_d\triangleq\eta_d-\hat{\eta}_d$, $\tilde{\eta}_q\triangleq\eta_q-\hat{\eta}_q$, and $\hat{\eta}_d$, $\hat{\eta}_q$ are the estimates of η_d, η_q, respectively.

3. DESIGN OF THE TORQUE AND FLUX CONTROLLER AND ERROR DYNAMICS

Based on the previously designed adaptive observer, we design two kinds of feedback linearization controllers for the torque and flux control of induction motors. Taking into account the mechanical outputs of induction motor and the power that is transformed into magnetic energy and then accumulated into the induction motor, etc, the estimates of motor torque and airgap flux can be obtained as follows.

$$\begin{aligned}\hat{T}_e&=\frac{3P}{2}(\hat{\lambda}_{da}i_{qs}-\hat{\lambda}_{qa}i_{ds}),\\|\hat{\lambda}_a|&=\hat{\lambda}_{da}^2+\hat{\lambda}_{qa}^2.\end{aligned}\quad(13)$$

Define the error between the reference torque and the torque estimate as e_1 and the error between estimated flux and its reference as e_2.

$$e_1=\hat{T}_e-T_{e\_ref},\quad(14)$$

$$\begin{aligned}e_2&=|\hat{\lambda}_a|-|\lambda_a|_{ref}\\&=\hat{\lambda}_{da}^2+\hat{\lambda}_{qa}^2-|\lambda_a|_{ref}.\end{aligned}\quad(15)$$

Differentiating these errors leads to

$$\frac{d}{dt}e_1=\frac{3P}{2}(i_{qs}\frac{d}{dt}\hat{\lambda}_{da}+\hat{\lambda}_{da}\frac{d}{dt}i_{qs}-i_{ds}\frac{d}{dt}\hat{\lambda}_{qa}-\hat{\lambda}_{qa}\frac{d}{dt}i_{ds})-\frac{d}{dt}T_{e\_ref},\quad(16)$$

$$\begin{aligned}\frac{d}{dt}e_2=&-\frac{2(L_{ls}-L_\sigma)}{L_\sigma}\hat{\lambda}_{da}V_{ds}-\frac{2(L_{ls}-L_\sigma)}{L_\sigma}\hat{\lambda}_{qa}V_{qs}+\frac{2(L_{ls}-L_\sigma)}{L_\sigma}\hat{R}_s(i_{ds}\hat{\lambda}_{da}+i_{qs}\hat{\lambda}_{qa})\\&-\frac{2L_{ls}}{L_rL_\sigma}\hat{R}_r\{(\hat{\lambda}_{da}-L_mi_{ds})\hat{\lambda}_{da}+(\hat{\lambda}_{qa}-L_mi_{qs})\hat{\lambda}_{qa}\}\\&-\frac{2L_{ls}(L_{ls}-L_\sigma)}{L_\sigma}\omega_r(i_{qs}\hat{\lambda}_{da}-i_{ds}\hat{\lambda}_{qa})-\dot{\lambda}_{ref}.\end{aligned}\quad(17)$$

By using (3) and (6), (16) can be rewritten as

$$\begin{aligned}\frac{d}{dt}e_1=&\frac{3P}{2}[-\frac{1}{L_\sigma}\{(L_{ls}-L_\sigma)i_{qs}+\hat{\lambda}_{qa}\}V_{ds}+\frac{1}{L_\sigma}\{(L_{ls}-L_\sigma)i_{ds}+\hat{\lambda}_{da}\}V_{qs}\\&-\frac{L_{ls}}{L_rL_\sigma}\hat{R}_r\{(\hat{\lambda}_{da}-L_mi_{ds})i_{qs}\end{aligned}\quad(18)$$

$$-(\hat{\lambda}_{qa}-L_m i_{qs})i_{ds}\}-\frac{L_{ls}}{L_\sigma}\omega_r(\hat{\lambda}_{qa}i_{qs}+\hat{\lambda}_{da}i_{ds})$$
$$-\frac{L_{ls}(L_{ls}-L_\sigma)}{L_\sigma}\omega_r(i_{ds}^2+i_{qs}^2)$$
$$-\frac{L_{ls}-L_\sigma}{L_\sigma}\omega_r(i_{ds}\hat{\lambda}_{da}+i_{ds}\hat{\lambda}_q)-\frac{R_s}{L_\sigma}(i_{qs}\hat{\lambda}_{da}-i_{ds}\hat{\lambda}_{qa})$$
$$+\frac{(\lambda_{qa}-L_m i_{qs})}{L_r L_\sigma}R_r\hat{\lambda}_{da}-\frac{(\lambda_{da}-L_m i_{ds})}{L_r L_\sigma}R_r\hat{\lambda}_{qa}$$
$$-\frac{\omega_r}{L_\sigma}(\lambda_{da}\hat{\lambda}_{da}+\lambda_{qa}\hat{\lambda}_{qa})]-\dot{T}_{e\_ref}.$$

By applying the feedback linearizing control approach to (17) and (18), the control inputs V_{ds}, V_{qs} is designed to satisfy the equation

$$-\frac{1}{L_\sigma}\{(L_{ls}-L_\sigma)i_{qs}+\hat{\lambda}_{qa}\}V_{ds}+\frac{1}{L_\sigma}\{(L_{ls}-L_\sigma)i_{ds}+\hat{\lambda}_{da}\}V_{qs}=g_{d1}+g_{d2}, \quad (19)$$

$$-\frac{2(L_{ls}-L_\sigma)}{L_\sigma}\hat{\lambda}_{da}V_{ds}-\frac{2(L_{ls}-L_\sigma)}{L_\sigma}\hat{\lambda}_{qa}V_{qs}=g_{q1}, \quad (20)$$

where g_{d1}, g_{d2}, and g_{q1} are designed in order to deal with some directly removable terms. g_{d1} and g_{q1} are designed as in (21) and (22), with c_1 and c_2 as positive value, while g_{d2} will be determined later. •

$$g_{d1}=\frac{L_{ls}}{L_r L_\sigma}\hat{R}_r\{(\hat{\lambda}_{da}-L_m i_{ds})i_{qs}-(\hat{\lambda}_{qa}-L_m i_{qs})i_{ds}\}$$
$$+\frac{L_{ls}}{L_\sigma}\omega_r(\hat{\lambda}_{qa}i_{qs}+\hat{\lambda}_{da}i_{ds})+\frac{L_{ls}(L_{ls}-L_\sigma)}{L_\sigma}\omega_r(i_{ds}^2+i_{qs}^2)$$
$$+\frac{L_{ls}-L_\sigma}{L_\sigma}\omega_r(i_{ds}\hat{\lambda}_{da}+i_{qs}\hat{\lambda}_{qa})+\frac{\hat{R}_s}{L_\sigma}(i_{qs}\hat{\lambda}_{da}-i_{ds}\hat{\lambda}_{qa})$$
$$-\frac{(\hat{\lambda}_{qa}-L_m i_{qs})}{L_r L_\sigma}\hat{R}_r\hat{\lambda}_{da}+\frac{(\hat{\lambda}_{da}-L_m i_{ds})}{L_r L_\sigma}\hat{R}_r\hat{\lambda}_{qa}$$
$$+\frac{\omega_r}{L_\sigma}(\hat{\lambda}_{da}^2+\hat{\lambda}_{qa}^2)-c_1e_1+\frac{2}{3P}\dot{T}_{e\_ref}. \quad (21)$$

$$g_{q1}=-\frac{2(L_{ls}-L_\sigma)}{L_\sigma}\hat{R}_s(i_{ds}\hat{\lambda}_{da}+i_{qs}\hat{\lambda}_{qa})$$
$$+\frac{2L_{ls}}{L_r L_\sigma}\hat{R}_r\{(\hat{\lambda}_{da}-L_m i_{ds})\hat{\lambda}_{da}+(\hat{\lambda}_{qa}-L_m i_{qs})\hat{\lambda}_{qa}\}$$
$$+\frac{2L_{ls}(L_{ls}-L_\sigma)}{L_\sigma}\omega_r(i_{qs}\hat{\lambda}_{da}-i_{ds}\hat{\lambda}_{qa})+\dot{\lambda}_{ref}-c_2e_2. \quad (22)$$

The equations (18), (19), and (21) yield

$$\frac{d}{dt}e_1=\frac{3P}{2}[-c_1e_1-\frac{\tilde{R}_s}{L_\sigma}(i_{qs}\hat{\lambda}_{da}-i_{ds}\hat{\lambda}_{qa}) \quad (23)$$
$$+\frac{R_r}{L_r L_\sigma}(\hat{\lambda}_{da}\lambda_{qa}-\hat{\lambda}_{qa}\lambda_{da})$$
$$+\frac{L_m\tilde{R}_r}{L_r L_\sigma}(i_{ds}\hat{\lambda}_{qa}-i_{qs}\hat{\lambda}_{da})$$
$$-\frac{\omega_r}{L_\sigma}(\hat{\lambda}_{da}\lambda_{da}+\hat{\lambda}_{qa}\lambda_{qa})+g_{d2}].$$

Similarly to the observer design, by using (9), (23) is expressed as

$$\frac{d}{dt}e_1=\frac{3P}{2}[-c_1e_1-\frac{\tilde{R}_s}{L_\sigma}\{(i_{qs}\hat{\lambda}_{da}-i_{ds}\hat{\lambda}_{qa})$$
$$-\omega_r(\hat{\lambda}_{da}I_{ds}+\hat{\lambda}_{qa}I_{qs})+\frac{L_m\tilde{R}_r}{L_r L_\sigma}(i_{ds}\hat{\lambda}_{qa}-i_{qs}\hat{\lambda}_{da})$$
$$+\frac{\omega_r}{L_\sigma}(L_{ls}\hat{\lambda}_{da}\tilde{i}_{ds}+L_{ls}\hat{\lambda}_{qa}\tilde{i}_{qs}+\hat{\lambda}_{da}\int_0^t\dot{\hat{R}}_s I_{ds}dt$$
$$+\hat{\lambda}_{qa}\int_0^t\dot{\hat{R}}_s I_{qs}dt)-\frac{\omega_r}{L_\sigma}(\hat{\lambda}_{da}z_d+\hat{\lambda}_{qa}z_q)$$
$$+\frac{R_r}{L_r L_\sigma}\hat{\lambda}_{da}\tilde{z}_q-\frac{R_r}{L_r L_\sigma}\hat{\lambda}_{qa}\tilde{z}_d$$
$$-\frac{R}{L_r L_\sigma}(\hat{\lambda}_{da}I_{qs}-\hat{\lambda}_{qa}I_{ds})+\frac{R_r}{L_r L_\sigma}\{\hat{\lambda}_{da}\hat{z}_q \quad (24)$$
$$-\hat{\lambda}_{qa}\hat{z}_d-L_{ls}(\hat{\lambda}_{da}\tilde{i}_{qs}+\hat{\lambda}_{qa}\tilde{i}_{ds})$$
$$+\hat{\lambda}_{da}\int_0^t\hat{R}_s i_{qs}dt-\hat{\lambda}_{qa}\int_0^t\hat{R}_s i_{ds}dt\}+g_{d2}].$$

By choosing g_{d2} as

$$g_{d2}=-\frac{\omega_r}{L_\sigma}(L_{ls}\hat{\lambda}_{da}\tilde{i}_{ds}+L_{ls}\hat{\lambda}_{qa}\tilde{i}_{qs}$$
$$+\hat{\lambda}_{da}\int_0^t\dot{\hat{R}}_s I_{ds}dt+\hat{\lambda}_{qa}\int_0^t\dot{\hat{R}}_s I_{qs}dt)$$
$$+\frac{\omega_r}{L_\sigma}(\hat{\lambda}_{da}\hat{z}_d+\hat{\lambda}_{qa}\hat{z}_q+\hat{\lambda}_{da}\hat{\eta}_d+\hat{\lambda}_{qa}\hat{\eta}_q) \quad (25)$$
$$+\frac{\hat{R}}{L_r L_\sigma}(\hat{\lambda}_{da}I_{qs}-\hat{\lambda}_{qa}I_{ds})-\frac{\hat{R}_r}{L_r L_\sigma}\{\hat{\lambda}_{da}\hat{z}_q$$
$$-\hat{\lambda}_{qa}\hat{z}_d-L_{ls}(\hat{\lambda}_{da}\tilde{i}_{qs}+\hat{\lambda}_{qa}\tilde{i}_{ds})$$
$$+\hat{\lambda}_{da}\int_0^t\hat{R}_s i_{qs}dt-\hat{\lambda}_{qa}\int_0^t\hat{R}_s i_{ds}dt\},$$

(24) can be rewritten as

$$\frac{d}{dt}e_1=\frac{3P}{2}[-c_1e_1-\frac{\tilde{R}_s}{L_\sigma}\{(i_{qs}\hat{\lambda}_{da}-i_{ds}\hat{\lambda}_{qa}) \quad (26)$$
$$-\omega_r(\hat{\lambda}_{da}I_{ds}+\hat{\lambda}_{qa}I_{qs})\}-\frac{\omega_r}{L_\sigma}\hat{\lambda}_{da}\tilde{\eta}_d$$

$$-\frac{\omega_r}{L_\sigma}\hat{\lambda}_{qa}\tilde{\eta}_q+\frac{R_r}{L_rL_\sigma}\hat{\lambda}_{da}\tilde{z}_q-\frac{R_r}{L_rL_\sigma}\hat{\lambda}_{qa}\tilde{z}_d$$
$$-\frac{\tilde{R}}{L_rL_\sigma}(\hat{\lambda}_{da}I_{qs}-\hat{\lambda}_{qa}I_{ds})+\frac{\tilde{R}_r}{L_rL_\sigma}\{L_m(i_{ds}\hat{\lambda}_{qa}$$
$$-i_{qs}\hat{\lambda}_{da})+(\hat{\lambda}_{da}\hat{z}_q-\hat{\lambda}_{qa}\hat{z}_d)-L_{ls}(\hat{\lambda}_{da}\tilde{i}_{qs}+\hat{\lambda}_{qa}\tilde{i}_{ds})$$
$$+\hat{\lambda}_{da}\int_0^t\hat{R}_si_{qs}dt-\hat{\lambda}_{qa}\int_0^t\hat{R}_si_{ds}dt\}].$$

The equations (17), (20), and (22) then yields

$$\frac{d}{dt}e_2=-c_2e_2 \tag{27}$$

which is globally asymptotically stable. The equations (26) and (27) will be used as error dynamics to design the adaptive law in the next section.

Accordingly, the two actual control input vector for torque and flux control in (19) and (20) can be rewritten in a vector form as follows.

$$\begin{bmatrix}(L_{ls}-L_\sigma)i_{qs}+\hat{\lambda}_{qa} & -(L_{ls}-L_\sigma)i_{ds}-\hat{\lambda}_{da}\\ (L_{ls}-L_\sigma)\hat{\lambda}_{da} & (L_{ls}-L_\sigma)\hat{\lambda}_{qa}\end{bmatrix}\begin{bmatrix}V_{ds}\\ V_{qs}\end{bmatrix}=-L_\sigma\begin{bmatrix}g_{d1}+g_{d2}\\ g_{q1}\end{bmatrix}. \tag{28}$$

4. ADAPTIVE LAW DESIGN AND CONVERGENCE ANALYSIS

In this section, the overall adaptive law is designed to achieve the asymptotical stability of the whole error dynamics including adaptive observer's estimation error, torque control error, and flux control error. The error dynamics in (12), (26), and (27) can be expressed in the following matrix form.

$$\dot{e}=Ae+W^T\tilde{\theta},$$
$$e=\begin{bmatrix}\tilde{i}_{ds} & \tilde{i}_{qs} & e_1 & e_2\end{bmatrix}^T,$$
$$\theta=\begin{bmatrix}R_s & R_r & R & z_d & z_q & \eta_d & \eta_q\end{bmatrix}^T,$$
$$\tilde{\theta}=\begin{bmatrix}\tilde{R}_s & \tilde{R}_r & \tilde{R} & \tilde{z}_d & \tilde{z}_q & \tilde{\eta}_d & \tilde{\eta}_q\end{bmatrix}^T,$$
$$A=\begin{pmatrix}-k_1-\frac{L_{ls}R_r}{L_rL_\sigma} & 0 & 0 & 0\\ 0 & -k_2-\frac{L_{ls}R_r}{L_rL_\sigma} & 0 & 0\\ 0 & 0 & -\frac{3P}{2}c_1 & 0\\ 0 & 0 & 0 & -c_2\end{pmatrix},$$

$$W^T=\begin{bmatrix}\frac{-(i_{ds}+\omega_rI_{qs})}{L_\sigma} & D_1 & -\frac{I_{ds}}{L_rL_\sigma} & \frac{R_r}{L_rL_\sigma} & 0 & 0 & \frac{\omega_r}{L_\sigma}\\ \frac{-(i_{qs}-\omega_rI_{ds})}{L_\sigma} & D_2 & -\frac{I_{qs}}{L_rL_\sigma} & 0 & \frac{R_r}{L_rL_\sigma} & -\frac{\omega_r}{L_\sigma} & 0\\ D_3 & D_4 & -\frac{(\hat{\lambda}_{da}I_{qs}-\hat{\lambda}_{qa}I_{ds})}{L_rL_\sigma} & -\frac{R_r}{L_rL_\sigma}\hat{\lambda}_{qa} & \frac{R_r}{L_rL_\sigma}\hat{\lambda}_{da} & -\frac{\omega_r}{L_\sigma}\hat{\lambda}_{da} & -\frac{\omega_r}{L_\sigma}\hat{\lambda}_{qa}\\ 0 & 0 & 0 & 0 & 0 & 0 & 0\end{bmatrix},$$

$$D_1=\frac{1}{L_rL_\sigma}\left\{\hat{\lambda}_{da}-L_mi_{ds}+\hat{z}_d+\frac{1}{L_\sigma}\int_0^t\hat{R}_si_{ds}dt\right\},$$
$$D_2=\frac{1}{L_rL_\sigma}\left\{\hat{\lambda}_{qa}-L_mi_{qs}+\hat{z}_q+\frac{1}{L_\sigma}\int_0^t\hat{R}_si_{qs}dt\right\},$$
$$D_3=-\frac{\left(i_{qs}\hat{\lambda}_{da}-i_{ds}\hat{\lambda}_{qa}\right)+\omega_r\left(\hat{\lambda}_{da}I_{ds}+\hat{\lambda}_{qa}I_{qs}\right)}{L_\sigma},$$
$$D_4=\frac{\{L_m(i_{ds}\hat{\lambda}_{qa}-i_{qs}\hat{\lambda}_{da})+(\hat{\lambda}_{da}\hat{z}_q-\hat{\lambda}_{qa}\hat{z}_d)}{L_rL_\sigma}$$
$$\frac{-L_{ls}(\hat{\lambda}_{da}\tilde{i}_{qs}+\hat{\lambda}_{qa}\tilde{i}_{ds})+\hat{\lambda}_{da}\int_0^t\hat{R}_si_{qs}dt-\hat{\lambda}_{qa}\int_0^t\hat{R}_si_{ds}dt\}}{L_rL_\sigma}. \tag{29}$$

The overall adaptation law by using Lyapunov's direct method, is proposed as

$$\dot{\tilde{\theta}}=-\Gamma We, \tag{30}$$

where $\Gamma=diag\left[L_\sigma\gamma_s\quad L_rL_\sigma\gamma_r\quad L_\sigma L_r\gamma_R\quad \frac{L_rL_\sigma}{R_r}\gamma_z\quad \frac{L_rL_\sigma}{R_r}\gamma_z\quad L_\sigma\gamma_\eta\quad L_\sigma\gamma_\eta\right]$, and γ_r, γ_s, γ_R, γ_z, γ_η are positive gains. Since R_s, R_r, R are fixed constants, $\dot{\tilde{R}}_s=-\dot{\hat{R}}_s$, $\dot{\tilde{R}}_r=-\dot{\hat{R}}_r$, $\dot{\tilde{R}}=-\dot{\hat{R}}$ hold. Considering $\dot{z}_d=-L_{ls}f_d$, $\dot{z}_q=-L_{ls}f_q$ from (8), the adaptation law for $\hat{\theta}$ is equivalently expressed as

$$\dot{\hat{\theta}}=\Gamma We+[0\ \ 0\ \ 0\ \ -L_{ls}f_d\ \ -L_{ls}f_q\ \ -\gamma_z(\tilde{i}_{ds}-\hat{\lambda}_{qa}e_1)\ \ -\gamma_z(\tilde{i}_{qs}-\hat{\lambda}_{da}e_1)]^T. \tag{31}$$

(31) can also be expressed in terms of each parameter as follows.

$$\begin{aligned}
\dot{\hat{R}}_s &= -\gamma_s\{(i_{ds}+\omega_r I_{qs})\tilde{i}_{ds}+(i_{qs}-\omega_r I_{ds})\tilde{i}_{qs} \\
&\quad +\{(i_{qs}\hat{\lambda}_{da}-i_{ds}\hat{\lambda}_{qa})-\omega_r(\hat{\lambda}_{da}I_{ds}+\hat{\lambda}_{qa}I_{qs})\}e_1\}, \\
\dot{\hat{R}}_r &= \gamma_r[\ (\hat{\lambda}_{da}-L_m i_{ds}+\hat{z}_d+\int_0^t \hat{R}_s i_{ds}dt)\tilde{i}_{ds} \\
&\quad +(\hat{\lambda}_{qa}-L_m i_{qs}+\hat{z}_q+\int_0^t \hat{R}_s i_{qs}dt)\tilde{i}_{qs} \\
&\quad +\{L_m(i_{ds}\hat{\lambda}_{qa}-i_{qs}\hat{\lambda}_{da})+(\hat{\lambda}_{da}\hat{z}_q-\hat{\lambda}_{qa}\hat{z}_d) \\
&\quad -L_{ls}(\hat{\lambda}_{da}\tilde{i}_{qs}+\hat{\lambda}_{qa}\tilde{i}_{ds})+\hat{\lambda}_{da}\int_0^t \hat{R}_s i_{qs}dt \\
&\quad -\hat{\lambda}_{qa}\int_0^t \hat{R}_s i_{ds}dt\}e_1], \\
\dot{\hat{R}} &= -\gamma_R\{(I_{ds}\tilde{i}_{ds}+I_{qs}\tilde{i}_{qs})+(\hat{\lambda}_{da}I_{qs}-\hat{\lambda}_{qa}I_{ds})e_1\}, \\
\dot{\hat{z}}_d &= -L_{ls}f_d+\gamma_z(\tilde{i}_{ds}-\hat{\lambda}_{qa}e_1), \\
\dot{\hat{z}}_q &= -L_{ls}f_q+\gamma_z(\tilde{i}_{qs}+\hat{\lambda}_{da}e_1), \\
\dot{\hat{\eta}}_d &= -\gamma_z(\tilde{i}_{ds}-\hat{\lambda}_{qa}e_1)-\gamma_\eta\omega_r(\tilde{i}_{qs}+\hat{\lambda}_{da}e_1), \\
\dot{\hat{\eta}}_q &= -\gamma_z(\tilde{i}_{qs}+\hat{\lambda}_{da}e_1)+\gamma_\eta\omega_r(\tilde{i}_{ds}-\hat{\lambda}_{qa}e_1).
\end{aligned} \tag{32}$$

The convergence of the overall error system is dealt with in Theorem 1 based on the following two Assumptions.

Assumption 1: Stator current, stator voltage, rotor flux, rotor velocity, and the integration of stator current, are bounded.

Assumption 2: For some positive a_1, a_2, reference signals $\omega_{ref}(t)$, $|\lambda_a|_{ref}(t)$ are bounded C^1 functions with bounded derivatives such that

$$\lim_{t\to\infty}\omega_{ref}(t)=a_1,\ \ |\lambda_s|_{ref}(t)\ge a_2>0,\ \ \forall t>0.$$

Remarks 1: In most cases, when the induction motor is in steady-state, the state currents i_{ds}, i_{qs} become sinusoidal signals. Therefore, after transient period, it is natural to assume that their integrations are bounded. If the input frequency of the motor is maintained to be equal to zero, the state currents are DC. So their integrations may diverge. In this case, the integration values can be saturated by controller or the adaptation can be held on temporarily.

Theorem 1: Under the Assumptions 1 and 2, if the estimates for flux and current are given in (6), the control inputs are generated by (28), and the overall adaptive law is given as (32), then

i) $\tilde{\theta}\in L_\infty$, $e=\begin{bmatrix}\tilde{i}_{ds} & \tilde{i}_{qs} & e_1 & e_2\end{bmatrix}^T\in L_\infty\cap L_2$, $\lim_{t\to\infty} e=0$.

ii) If the persistent excitation condition is satisfied, the equilibrium point $\tilde{\theta}=\begin{bmatrix}\tilde{R}_s & \tilde{R}_r & \tilde{R} & \tilde{z}_d & \tilde{z}_q & \tilde{\eta}_d & \tilde{\eta}_q\end{bmatrix}^T=0$ is asymptotically stable (i.e., $\lim_{t\to\infty}\tilde{\theta}=0$).

iii) $\left|T_e-\hat{T}_e\right|\in L_\infty$, $|\lambda_a|-|\hat{\lambda}_a|\in L_\infty$. Furthermore, if the persistent excitation condition is satisfied, then $\lim_{t\to\infty}\tilde{R}_r=0$, $\lim_{t\to\infty}\tilde{R}_s=0$, $\lim_{t\to\infty}(T_e-T_{e\_ref})=0$, $\lim_{t\to\infty}(|\lambda_a|-|\lambda_a|_{ref})=0$, $\lim_{t\to\infty}\tilde{\lambda}_{dr}=0$, $\lim_{t\to\infty}\tilde{\lambda}_{qr}=0$.

Proof:

i) Define a Lyapunov function candidate and its derivative as follows.

$$\begin{aligned}
V &= \frac{1}{2}e^T e+\frac{1}{2}\tilde{\theta}^T\Gamma^{-1}\tilde{\theta}, \\
\frac{d}{dt}V &= \frac{1}{2}\{e^T\dot{e}+\dot{e}^T e\}+\frac{1}{2}\{\tilde{\theta}^T\Gamma^{-1}\dot{\tilde{\theta}}++\dot{\tilde{\theta}}^T\Gamma^{-1}\tilde{\theta}\} \\
&= e^T Ae+\tilde{\theta}^T We+\tilde{\theta}^T\Gamma^{-1}\dot{\tilde{\theta}}.
\end{aligned}$$

Applying (30) leads to

$$\frac{d}{dt}V=e^T Ae\le 0.$$

Therefore, $e=\begin{bmatrix}\tilde{i}_{ds} & \tilde{i}_{qs} & e_1 & e_2\end{bmatrix}^T\in L_\infty\cap L_2$, $\tilde{\theta}\in L_\infty$. Next, we show that W is bounded. Considering (15), we obtain $\hat{\lambda}_{da}\in L_\infty$, $\hat{\lambda}_{qa}\in L_\infty$. From the fact that R_s, $\tilde{R}_s$, R_r, $\tilde{R}_r\in L_\infty$, we obtain $\hat{R}_s$, $\hat{R}_r\in L_\infty$. From (2) and Assumption 1, $\lambda_{da}\in L_\infty$, $\lambda_{qa}\in L_\infty$. So, $\tilde{\lambda}_{qa}$, $\tilde{\lambda}_{da}\in L_\infty$ holds. From (8) and Assumption 1, z_d, $z_q\in L_\infty$. Since $\tilde{\theta}\in L_\infty$ means $\tilde{z}_d, \tilde{z}_q\in L_\infty$, we obtain $\hat{z}_d$, $\hat{z}_q\in L_\infty$. Therefore, D_1, D_2, D_3, D_4 $\in L_\infty$. Now by using Assumptions 1 and 2, and the fact that $D_1, D_2, D_3, D_4\in L_\infty$, W is bounded. $\dot{e}$ is also bounded by (29). Barbalat's Lemma [20] is then applied to obtain $\lim_{t\to\infty}e=0$.

ii) Refer to [20, pp. 367-370].

iii) The relation (33) shows $\left|T_e-\hat{T}_e\right|\in L_\infty$, $|\lambda_a|-|\hat{\lambda}_a|\in L_\infty$.

$$\begin{aligned}
T_e-\hat{T}_e &= \frac{3P}{2}(i_{qs}\tilde{\lambda}_{da}-i_{ds}\tilde{\lambda}_{qa}), \\
|\lambda_a|-|\hat{\lambda}_a| &= \tilde{\lambda}_{da}(\lambda_{da}+\hat{\lambda}_{da})+\tilde{\lambda}_{qa}(\lambda_{qa}+\hat{\lambda}_{qa}).
\end{aligned} \tag{33}$$

If persistent excitation condition is satisfied, $\tilde{R}_r = 0$, $\tilde{R}_s = 0$ hold by ii), and applying this to (7) leads to

$$\frac{d}{dt}\tilde{\lambda}_{qa} = -\frac{L_{ls}}{L_r L_\sigma} R_r \tilde{\lambda}_{qa} + \frac{L_{ls}}{L_\sigma}\omega_r \tilde{\lambda}_{da}. \tag{34}$$

Define Lyapunov-like function candidate as $V_a = \frac{1}{2}\left(\tilde{\lambda}_{da}^2 + \tilde{\lambda}_{qa}^2\right)$. Then its derivative is $\frac{d}{dt}V_a = -\frac{L_{ls}R_r}{L_r L_\sigma}\left(\tilde{\lambda}_{da}^2 + \tilde{\lambda}_{qa}^2\right)$.

Therefore, $\left[\tilde{\lambda}_{da}, \ \tilde{\lambda}_{qa}\right] \in L_\infty \cap L_2$. Since $\dot{\tilde{\lambda}}_{da}$ and $\dot{\tilde{\lambda}}_{qa}$ are also bounded from (34), $\lim_{t\to\infty}\tilde{\lambda}_{da} = 0$, $\lim_{t\to\infty}\tilde{\lambda}_{qa} = 0$ is obtained by using Barbalat's Lemma [20]. Therefore, by using (33), $\lim_{t\to\infty}(T_e - \hat{T}_e) = 0$ and $\lim_{t\to\infty}(|\lambda_a| - |\hat{\lambda}_a|) = 0$. Since $\lim_{t\to\infty} e_1 = \lim_{t\to\infty}(T_e - \hat{T}_e) = 0$ and $\lim_{t\to\infty} e_2 = \lim_{t\to\infty}(|\hat{\lambda}_a| - \lambda_{ref}) = 0$ in i), $\lim_{t\to\infty}(T_e - T_{e\_ref}) = 0$ and $\lim_{t\to\infty}(|\lambda_a| - \lambda_{ref}) = 0$ are obtained. □

In order to prevent the rotor and stator resistances from becoming negative, the projection algorithm is used as

$$\dot{\hat{R}}_{r,p} = \begin{cases} \dot{\hat{R}}_r & \text{if } \hat{R}_{r,p} > 0, \\ & \text{or if } \hat{R}_{r,p} = 0 \text{ and } \dot{\hat{R}}_r \geq 0, \\ 0 & \text{if } \hat{R}_{r,p} = 0 \text{ and } \dot{\hat{R}}_r \leq 0, \end{cases}$$
$$\dot{\hat{R}}_{s,p} = \begin{cases} \dot{\hat{R}}_s & \text{if } \hat{R}_{s,p} > 0, \\ & \text{or if } \hat{R}_{s,p} = 0 \text{ and } \dot{\hat{R}}_s \geq 0, \\ 0 & \text{if } \hat{R}_{s,p} = 0 \text{ and } \dot{\hat{R}}_s \leq 0, \end{cases} \tag{35}$$
$$\dot{\hat{R}}_{p} = \begin{cases} \dot{\hat{R}} & \text{if } \hat{R}_{p} > 0, \\ & \text{or if } \hat{R}_{p} = 0 \text{ and } \dot{\hat{R}} \geq 0, \\ 0 & \text{if } \hat{R}_{p} = 0 \text{ and } \dot{\hat{R}} \leq 0. \end{cases}$$

By using this algorithm, the estimates of stator and rotor resistances are maintained as non-negative values.

Remarks 2: Simulation results will show that the persistent excitation condition is actually satisfied. Since W^T contains the signals i_{ds}, i_{qs}, persistence excitation condition requires that the frequency of i_{ds}, i_{qs} is sufficiently rich, making the rows of W^T to be independent of one another in the interval $[t, t+T]$. The first five rows of W^T are independent because of the currents with sufficiently rich frequency, while the remaining two each row needs at least one oscillation in the interval $[t, t+T]$, to be independent of each other.

Remarks 3: If motor velocity ω_r is constant, $\int WW^T dt$ cannot be guaranteed to be positive definite. In this case, we need the following extended persistent excitation condition. Define new variables as

$$\xi_d = \frac{R_r}{L_r L_\sigma}\tilde{z}_d + \frac{\omega_r}{L_\sigma}\tilde{\eta}_q,$$
$$\xi_q = \frac{R_r}{L_r L_\sigma}\tilde{z}_q - \frac{\omega_r}{L_\sigma}\tilde{\eta}_d. \tag{36}$$

By using the adaptive law (30), the error dynamics is

$$\frac{d}{dt}\xi_d = -(\gamma_z \frac{R_r}{L_r L_\sigma} + \gamma_\eta \frac{\omega_r^2}{L_\sigma})(\tilde{i}_{ds} - \hat{\lambda}_{qa} e_1),$$
$$\frac{d}{dt}\xi_q = -(\gamma_z \frac{R_r}{L_r L_\sigma} + \gamma_\eta \frac{\omega_r^2}{L_\sigma})(\tilde{i}_{qs} - \hat{\lambda}_{da} e_1). \tag{37}$$

Now (29) can be rewritten by using ξ_d, ξ_q as

$$\dot{e} = Ae + W_\xi^T \tilde{\theta}_\xi,$$
$$\tilde{\theta}_\xi = \left[\tilde{R}_s \ \ \tilde{R}_r \ \ \tilde{R} \ \ \xi_d \ \ \xi_q\right]^T, \tag{38}$$
$$W_\xi^T = \begin{bmatrix} \frac{-\left(i_{ds} + \omega_r I_{qs}\right)}{L_\sigma} & D_1 & -\frac{I_{ds}}{L_r L_\sigma} & 1 & 0 \\ \frac{-\left(i_{qs} - \omega_r I_{ds}\right)}{L_\sigma} & D_2 & -\frac{I_{qs}}{L_r L_\sigma} & 0 & 1 \\ D_3 & D_4 & -\frac{(\hat{\lambda}_{da} I_{qs} - \hat{\lambda}_{qa} I_{ds})}{L_r L_\sigma} & -\hat{\lambda}_{qa} & \hat{\lambda}_{da} \\ 0 & 0 & 0 & 0 & 0 \end{bmatrix}$$

where D_1, D_2, D_3, D_4 are the same as in (29). If there exist $T > 0$, $c > 0$, such that $\int_t^{t+T} W_\xi(\tau) W_\xi^T(\tau) d\tau \geq cI > 0$ for any $t > 0$, $\tilde{\theta}_\xi$ is guaranteed to converge to zero. In other words, if ω_r is constant, it is not guaranteed that $\tilde{z}_d$, $\tilde{z}_q$, $\tilde{\eta}_d$, $\tilde{\eta}_q$ converge to zero. But if the persistent excitation of W_ξ is satisfied, the convergence of $\tilde{R}_r$, $\tilde{R}_s$, $\tilde{R}$ is guaranteed. If $\tilde{R}_r = \tilde{R}_s = 0$, the flux converges to its actual value, and its magnitude and torque also track their reference values, by iii) in Theorem 1.

5. SIMULATIONS

Table 1 shows the motor specification used in the simulation. We used a PI controller for speed control and the output of the torque reference was applied to the controller. The initial error of the rotor resistance and stator resistance were set to -50% and +50%, respectively. The reference value of speed was increased up to 1800r/min at 0.2s. The simulation results, as shown in Fig. 1, demonstrate that as the stator current error and airgap flux error converged to zero with properly bounded voltages (See Fig. 1(e), 1(d) and 1(f)), the resistances of stator and rotor converged to their actual values(See Fig. 1(c)), Torque

Table 1. Induction motor specification.

400W, 220V, 60Hz, 4 poles, max-speed 1690r/min			
R_s	3.3 Ω	L_m	99.0 mH
R_r	3.1 Ω	J	0.003 kgm^2
L_s	104.4 mH	Max-flux	0.45 Wb
L_r	104.4 mH	Max-torque	2.2 Nm

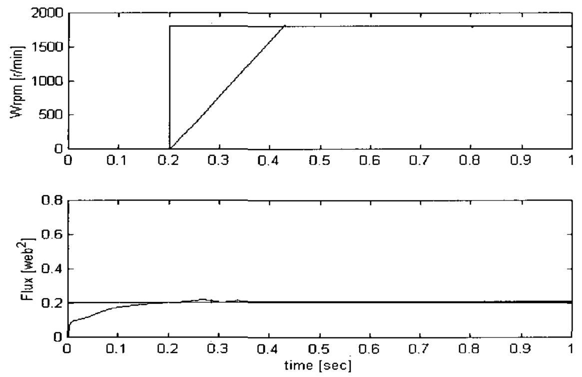

(a) References and actual values of motor-velocity (ω_{rpm}), magnitude of flux $(|\lambda_a|)$.

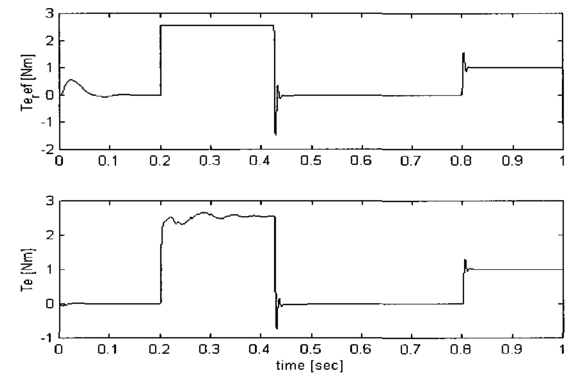

(b) Torque reference (T_{e_ref}) and actual torque T_e.

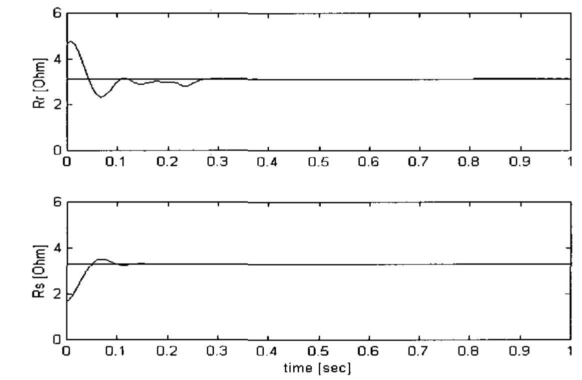

(c) Estimates of rotor resistance $(\hat{R}_r)$ and stator resistance $(\hat{R}_s)$.

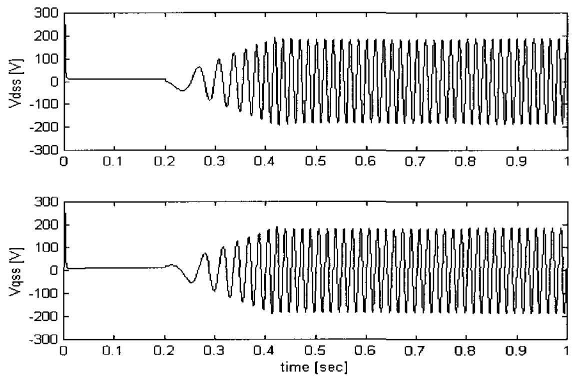

(d) d, q-axis voltage.

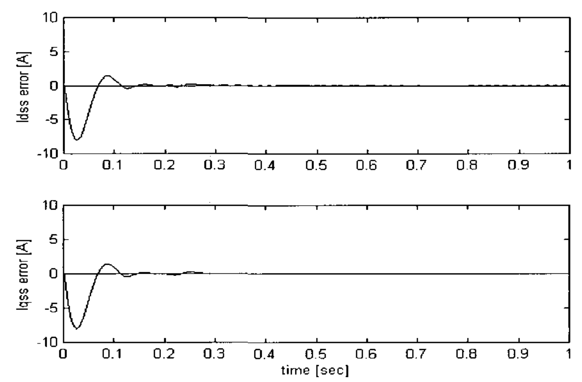

(e) d, q-axis current error $(\tilde{i}_{ds}, \tilde{i}_{qs})$.

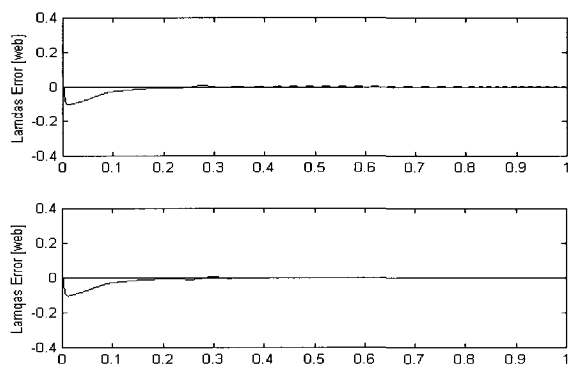

(f) Airgap flux error $(\tilde{\lambda}_{da}, \tilde{\lambda}_{qa})$.

Fig. 1. Simulation results of the proposed adaptive input-output feedback linearization controller $(\hat{R}_r(0) = R_r \times 1.5,\ \hat{R}_s(0) = R_s \times 0.5)$.

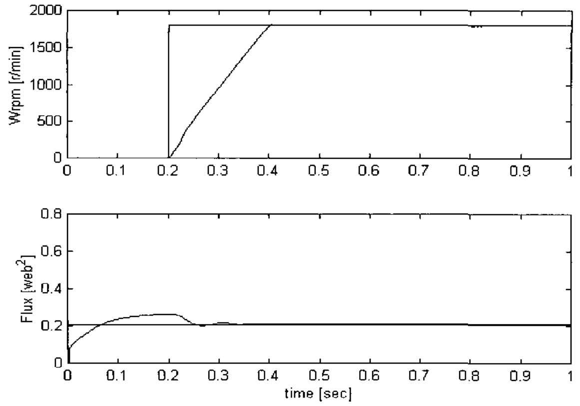

(a) References and actual values of motor-velocity (ω_{rpm}), magnitude of flux ($|\lambda_a|$).

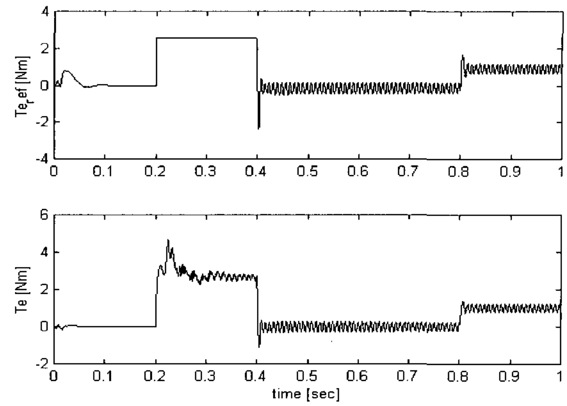

(b) Torque reference (T_{e_ref}) and actual torque (T_e).

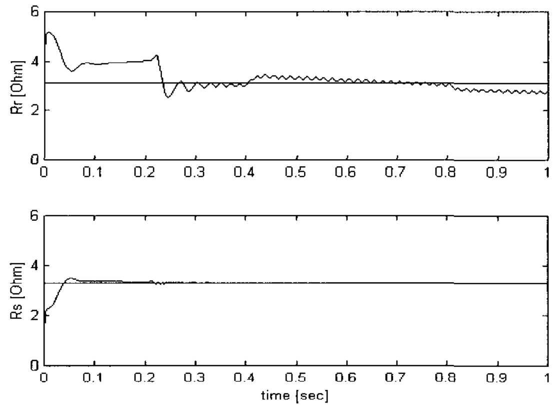

(c) Estimates of rotor resistance ($\hat{R}_r$) and stator resistance ($\hat{R}_s$).

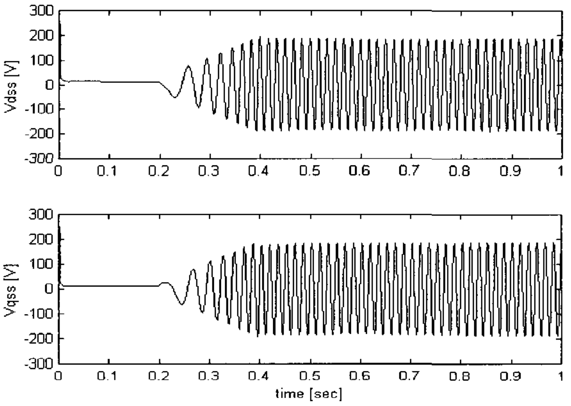

(d) d, q-axis voltage.

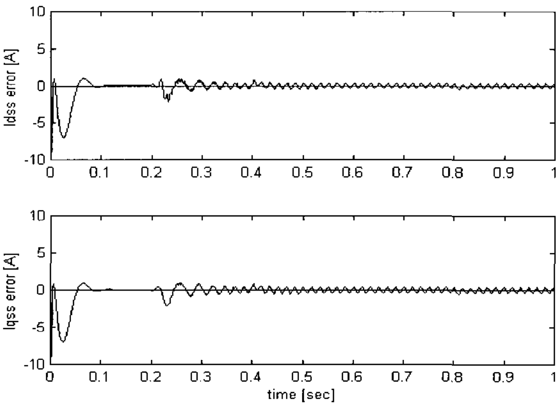

(e) d, q-axis current error ($\tilde{i}_{ds}$, $\tilde{i}_{qs}$).

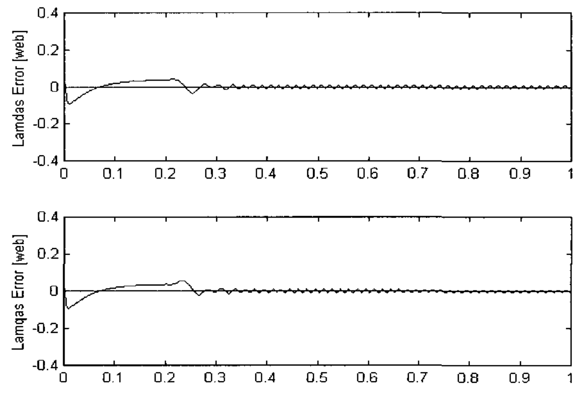

(f) Airgap flux error ($\tilde{\lambda}_{da}$, $\tilde{\lambda}_{qa}$).

Fig. 2. Simulation results of the proposed adaptive input-output feedback linearization controller (inductance error: $0.9\times L_m$, $0.9\times L_{ls}$, $0.5\times L_{lr}$, Initial resistance erros: $\hat{R}_r(0)=R_r\times 1.5$, $\hat{R}_s(0)=R_s\times 0.5$).

was controlled efficiently (See Fig. 1(b)), and the speed and flux converged to their reference values (See Fig. 1(a)).

With the exception of rotor and resistance errors, there may be in fact additional errors in real control systems. If the proposed control algorithm fails due to a slight change of some other parameters or system uncertainties, it shall be said to have very low reliability. In Fig. 2, small changes were made to mutual inductance (L_m), stator leakage inductance (L_{ls}) and rotor leakage inductance (L_{lr}) in order to confirm whether the proposed algorithm works well with the uncertainties of other parameters. In other words, 0.9* L_m, 0.9×L_{ls}, 0.9×L_{lr} were adopted to the system,

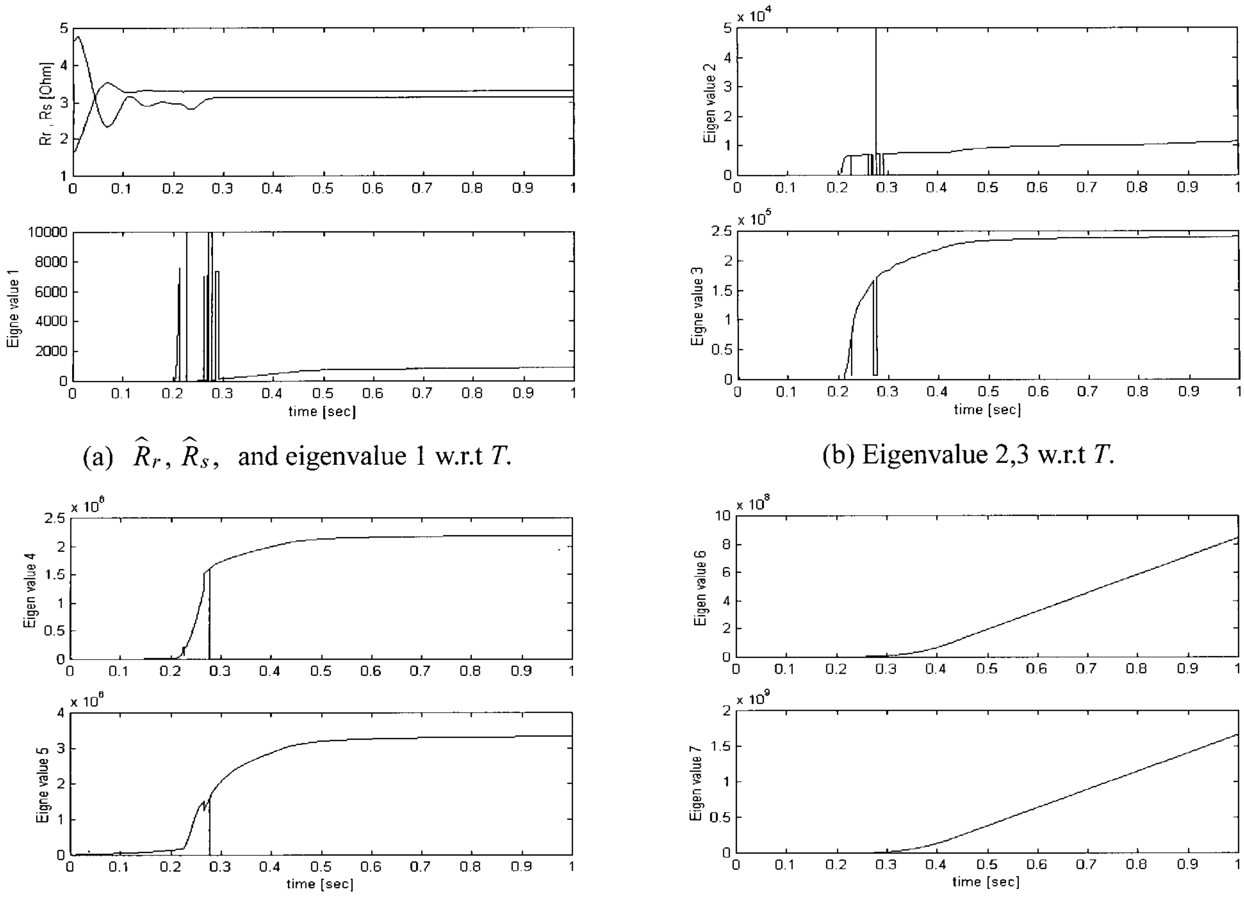

(a) $\hat{R}_r$, $\hat{R}_s$, and eigenvalue 1 w.r.t T.

(b) Eigenvalue 2,3 w.r.t T.

(c) Eigenvalue 4,5 w.r.t T.

(d) Eigenvalue 6,7 w.r.t T.

Fig. 3. Persistent excitation condition test.

instead of L_m, L_{ls}, L_{lr}, and the same controller was applied. It was founded that the *d-q* axis current errors $(\tilde{i}_{ds}, \tilde{i}_{qs})$ do not converge but oscillate (See Fig. 2(e)), and rotor resistance $(\hat{R}_r)$ does not track its actual value (See Fig. 2(c)). This is a natural outcome for model uncertainty, but as shown in Figs. 2(a) and 2(b), the velocity and torque are controlled independently with slight oscillation, in spite of the inductance errors. Airgap fluxes were also estimated well, even though there was oscillation. Some speed error existed near 0s, which was not seen in simulations due to scaling. The reason for the speed error is that flux and torque controller is not decoupled completely because of modeling mismatches of R_s, R_r initial errors, or inductance errors. Based on the results shown in Fig. 2, it is shown that the proposed control scheme is applicable to actual systems with some inductance uncertainties.

Now we will present our simulation results that show whether or not the persistent excitation condition can be satisfied. Since it is very difficult to test the persistent excitation condition analytically, we tested whether $\int_t^{t+T} W(\tau)W^T(\tau)d\tau$ remains positive definite for any $t > 0$. In this simulation, the eigenvalues of $\int_t^{t+T} W(\tau)W^T(\tau)d\tau$ with $t = 0$ actually remained positive over $T = [0,1]$ (See Fig. 3). As can be seen from Fig. 3, Some eigenvalues looks like they are close to zero, but, considering the scaling, they are actually positive.

Therefore $\int_t^{t+T} W(\tau)W^T(\tau)d\tau$ is positive definite, which in turn brings us to the conclusion that the persistent excitation condition is satisfied in the simulation.

6. EXPERIMENTS

In the experiment, two induction motors were used in the same way as in the simulation in order to evaluate the practical efficiency of the proposed controller. The sampling period of torque and flux controller was 200us, that of speed controller was 3ms the inverter switching frequency was 2.5Khz, the dc-link voltage was 310V, and DSP was TMS320C40 which has 40MFLOPS (mega floating point operation per second). As shown in Fig. 4, the proposed method

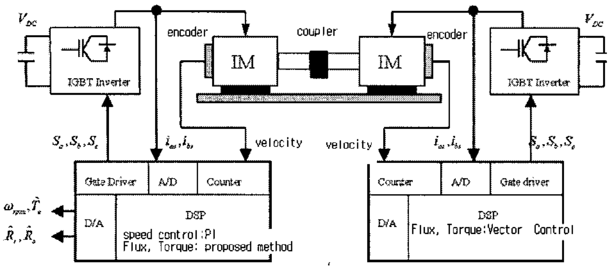

Fig. 4. Experimental environment for the evaluation of the proposed method.

was used for the left motor, while the direct-vector control method was used for the right one to generate load torque. The load torque 1Nm was applied at 1.4s to see load response in experiment. Experimental results are presented in Figs. 5. and 6.

Fig. 5 presents the experimental results where there exist no initial errors about rotor and stator resistances. Initial motor velocity reference is 0r/min and is increased up to 500r/min with 3r/min of slope. It can be seen from this figure that the estimates of the resistances do not go far from their actual values, and the velocity and torque are successfully controlled.

In Fig. 6, the situation is worse. There is stator resistance error of -50% (i.e. $\hat{R}_r(0) = R_r \times 0.5$), rotor resistance error of +50% (i.e. $\hat{R}_s(0) = R_s \times 1.5$), and mutual inductance error of +10% (i.e. $1.1L_m$). In addition, the velocity and torque controller works fairly well, while the estimates of the resistances of the stator and the rotor converge to their actual values, in spite of the initial errors.

When the mutual inductance error was increased further, the control failed as expected. But this is the kind of problem that can be observed in any control scheme that uses induction motor models. In order to

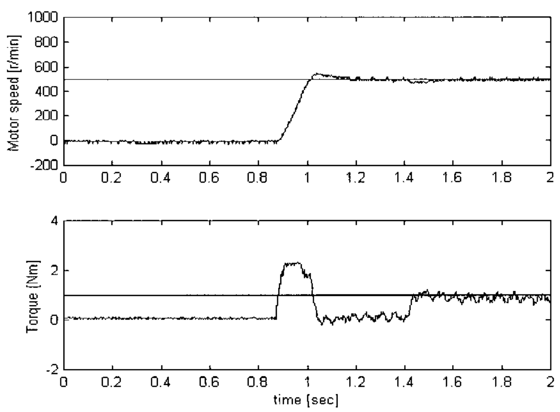

(a) References and actual values of motor velocity (ω_{rpm}) and estimate of torqe ($\hat{T}_e$).

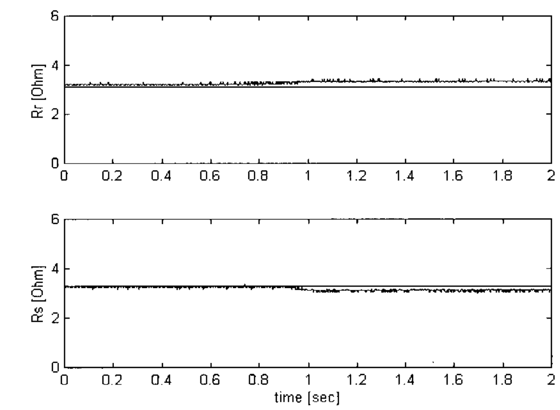

(b) Estimates of rotor resistance ($\hat{R}_r$) and stator resistance ($\hat{R}_s$).

Fig. 5. Experimental results of the adaptive input-output linearization controller with no initial errors ($\hat{R}_r(0) = R_r$, $\hat{R}_s(0) = R_s$).

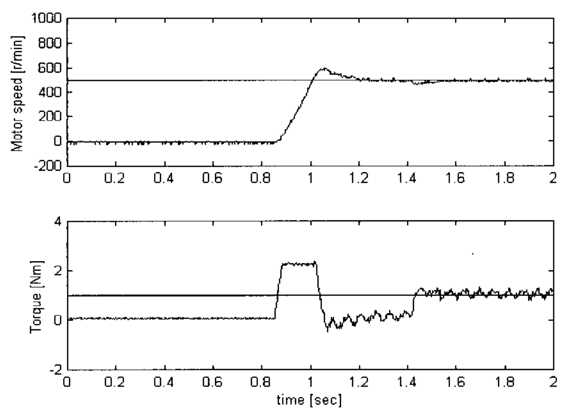

(a) References and actual values of motor velocity (ω_{rpm}) and estimate of torqe ($\hat{T}_e$).

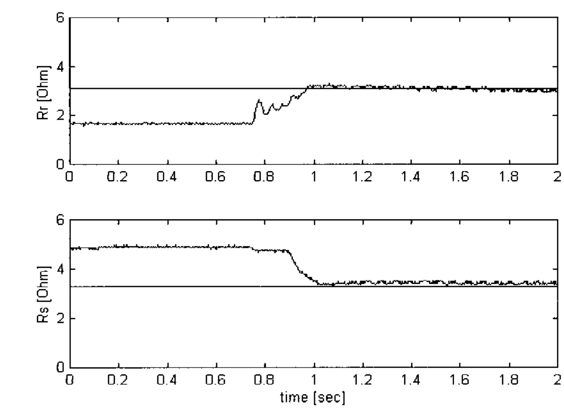

(b) Estimates of rotor resistance ($\hat{R}_r$) and stator resistance ($\hat{R}_s$).

Fig. 6. Experimental results of the adaptive input-output linearization controller with initial errors ($\hat{R}_r(0) = R_r \times 0.5$, $\hat{R}_s(0) = R_s \times 1.5, 1.1L_m$).

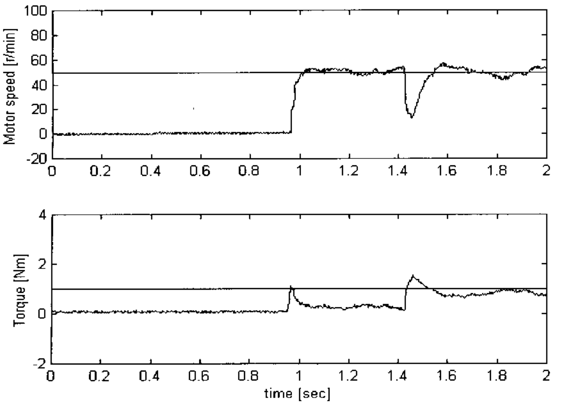

(a) References and actual values of motor velocity (ω_{rpm}) and estimate of torqe ($\hat{T}_e$).

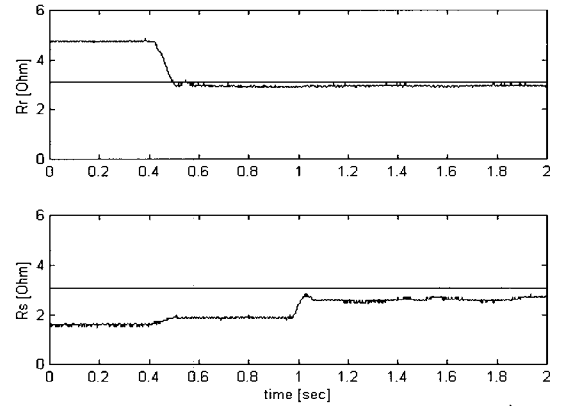

(b) Estimates of rotor resistance ($\hat{R}_r$) and stator resistance ($\hat{R}_s$).

Fig. 7. Low-Speed experimental results of the adaptive input-output linearization controller with initial errors ($\hat{R}_r(0) = R_r \times 0.5$, $\hat{R}_s(0) = R_s \times 1.5$, 1.1 L_m).

validate the efficiency of the controller at low speed operation, therefore, motor velocity was reduced to 50r/min. The results are shown in Fig. 7. It can be seen that the control works, but there still exist steady-state estimation errors. This is due to the stator voltage error which is relatively high at low speed operation. These experimental results show that the proposed scheme can be adopted into actual plants.

7. CONCLUSION

In this paper, we proposed an adaptive feedback linearization control scheme for induction motors with unknown rotor and stator resistances. Since the two existing typical modeling techniques, i.e., rotor flux model and stator flux model, entails structural complexities when they are combined into an overall control system with adaptive observer and feedback-linearizing controller, we proposed an airgap fluxe model to overcome this problem.

We developed a successful controller and observer design method that shows relatively less structural complexity. The feedback-linearizing controllers for torque and flux control were designed and then merged to derive the overall adaptive law taking into consideration all the error dynamics. This adaptive law was analyzed to show overall convergence. Through Lyapunov-based theoretical analysis, computer simulation, and actual experiments, we were able to demonstrate that the estimates of stator and rotor resistances converge to their actual values, flux is estimated efficiently, and torque and flux can be controlled independently. The convergence analysis were performed under persistent excitation condition and this condition was actually satisfied in simulations. These results confirm that the proposed adaptive feedback linearization control scheme is applicable both in theoretical and practical senses.

REFERENCES

[1] F. Blaschke, "The principle of field orientation applied to the new transvector closed-loop control system for rotating field machines," *Siemens-Rev.*, vol. 39, pp. 217-220, 1972.

[2] P. Vas, *Electrical Machines and Drives*, Clarendon Press, Oxford, 1992.

[3] X. Xu, R. De Doncker, and D. W. Novotny, "A stator flux oriented induction machine drive," *Proc. of PESC*, pp. 870-876,1988.

[4] W. L. Erdman and R. G. Hoft, "Induction machine field orientation along airgap and stator flux," *IEEE Trans. on Energy Conversion*, vol. 5, no. 1, pp. 115-120, 1990.

[5] X. Xu and D. W. Novotny, "Implementation of direct stator flux orientation control on a versatile DSP based system," *IEEE Trans. Ind. Applicat.*, vol. 27, no. 4, pp. 694-700, 1991.

[6] T. G. Habetler, F. Profumo, G. Griva, M. Pastorelli, and A. Bettini, "Stator resistance tuning in a stator-flux field-oriented drive using an instantaneous hybrid flux estimator," *IEEE Tran. on Power Electronics*, vol. 13, no. 1, pp. 125-133, 1998.

[7] Z. Krzeminski, "Nonlinear feedback and control strategy of the induction motor," *Proc. of IFAC Nonlin. Contr. Systems Design Sympos.*, Bordeaux, France, pp. 162-167, 1992.

[8] A. De Luca and G. Ulvi, "Design of exact nonlinear controller for induction motors," *IEEE Trans. Automat. Contr.*, vol. 34, no. 12, pp. 1304-1307, Dec. 1989.

[9] D.-I. Kim, I.-J. Ha, and M.-S. Ko, "Control of induction motors via feedback lineariation with input-output decoupling," *Int. J. Contr.*, vol. 51, pp. 863-883, 1990.

[10] R. Marino, S. Peresada, and P. Valigi, "Adaptive

input-output linearizing control of induction motors," *IEEE Trans. Automat. Contr.*, vol. 38, no. 2, pp. 208-221, 1993.

[11] Th. Von Raumer, J. M. Dion, L. Dugard, and J. L. Thomas, "Applied nonlinear control of an induction motor using digital signal processing," *IEEE Trans. Contr. Syst. Technol.*, vol. 2, no. 4, pp. 327-335, 1994.

[12] R. Marino, S. Peresada, and P. Tomei, "Output feedback control of current-fed induction motors with unknown rotor resistance," *IEEE Trans. Contr. Syst. Technol.*, vol. 4, no. 4, pp. 336-346, 1996.

[13] R. Marino, S. Peresada, and P. Tomei, "Adaptive observer-based control of induction motors with unknown rotor resistance," *Int. J. Adaptive Contr. Signal Proc.*, vol. 10, pp. 345-363, 1996.

[14] J. Chiasson, "A new approach to dynamic feedback linearization control of an induction motor," *IEEE Trans. Automat. Contr.*, vol. 43, no. 3, pp. 391-396, 1998.

[15] R. Marino, S. Peresada, and P. Tomei, "Global adaptive output feedback control of induction motors with uncertain rotor resistance," *IEEE Trans. Automat. Contr.*, vol. 44, no. 5, pp. 967-983, 1999.

[16] R. Ortega, P. Nicklasson, and G. Espinosa, "On speed control of induction motors," *Automatica*, vol. 32, no. 3, pp. 455-460, 1996.

[17] G. Espinosa-Perez and R. Ortega, "An output feedback globally stable controller for induction motors," *IEEE Trans. Automat. Contr.*, vol. 40, no. 1, pp. 138-143, 1995.

[18] K.-C. Kim, R. Ortega, and J.-P. Vilaino, "Theoretical and experimental comparison of two nonlinear controller for current-fed induction motors," *IEEE Trans. Contr. Syst. Technol.*, vol. 5, no. 3, pp. 338-347, 1997.

[19] I. Kanellakopoulos, P. T. Krein, and F. Disilvestro, "Nonlinear flux-observer-based control of induction motor," *Proc. of American Control Conf.*, Chicago, IL., pp. 1700-1704, 1992.

[20] R. Marino and P. Tomei, *Nonlinear Control Design - Geometric, Adaptive and Robust*, Prentice-Hall, Englewood Cliffs, NJ, 1995.

[21] G. C. Verghese and S. R. Sanders, "Observers for flux estimation in induction machines," *IEEE Trans. on Industrial Electronics*, vol. 35, no. 1, pp. 85-94, 1988.

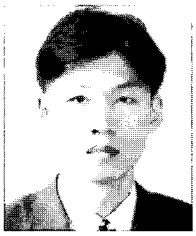

Seok Ho Jeon received the B.S., M.S., and Ph.D. degrees in Electrical Engineering from Seoul National University, Seoul, Korea in 1995, 1997, and 2002, respectively. His fields of interests are applications of modern control theory in electro-mechanical systems.

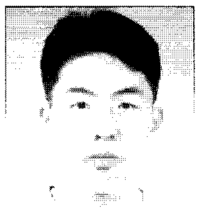

Dane Baang received the B.S. and M.S. degrees in Electrical Engineering from Korea University in 1999 and 2002, respectively. He is now a Ph.D. student in School of Electrical Engineering and Computer Science in Seoul National University. His research interest includes adaptive control and observer design, RHPTC, nonlinear control, and digital control.

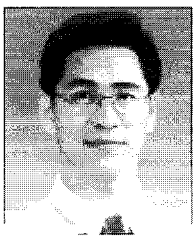

Jin Young Choi received the B.S., M.S., and Ph.D. degrees in Control and Instrumentation Engineering from Seoul National University in 1982, 1984, and 1993, respectively. He is now a Professor of School of Electrical Engineering and Computer Science in Seoul National University. His research interest includes neuro computing and control, adaptive and switching control, and cognitive vision.